[Research Paper] 대한금속·재료학회지 (*Korean J. Met. Mater.*), Vol. 56, No. 7 (2018) pp.524-531
DOI: 10.3365/KJMM.2018.56.7.524

Hydrogen Storage Properties of Mg-Graphene Composites

Myoung Youp Song[1,*], Young Jun Kwak[1], and Eunho Choi[2]

[1]*Division of Advanced Materials Engineering, Hydrogen & Fuel Cell Research Center, Engineering Research Institute, Chonbuk National University, Jeonju 54896, Republic of Korea*
[2]*Department of Materials Engineering, Graduate School, Chonbuk National University, Jeonju 54896, Republic of Korea*

Abstract: To improve the hydrogen uptake and release properties of magnesium (Mg), five weight percent of graphene was added to pre-milled Mg by milling in hydrogen (reaction-involving milling). The hydrogen uptake and release properties of the graphene-added Mg (named Mg-5graphene) were investigated. Pre-milling of Mg (for 24 h) and then adding graphene by milling in hydrogen (for 30 min) significantly increased the hydrogen uptake and release rates and the quantities of hydrogen absorbed and released for 60 min of the Mg and graphene composite. The activation of Mg-5graphene was completed after the second hydrogen uptake-release cycle (n=2). Mg-5graphene had a high effective hydrogen-storage capacity (quantity of hydrogen absorbed for 60 min) of 5.47 wt% at 593 K in 12 bar H_2 at n=3. Mg-5graphene absorbed 0.92 wt% H for 2.5 min, 2.67 wt% H for 10 min, and 5.62 wt% H for 60 min in 12 bar H_2 and released 0.25 wt% H for 2.5 min and 4.99 wt% H for 60 min in 1.0 bar H_2 at 623 K at n=1. The increase in I_D/I_G, the ratio of intensities of D and G peaks in Raman spectra, after reaction-involving milling of the pre-milled Mg with graphene, compared with that of the used graphene, suggests that defects and disordering in the graphene were increased. We believe that the generation of stacking fault disorder and formation of turbostratic graphite occurred after milling with the pre-milled Mg, rather than the formation of defects, in graphene.

(Received April 30, 2018; Accepted June 8, 2018)

Keywords: hydrogen absorbing materials, mechanical milling, hydrogen, microstructure, graphene-added Mg alloy

1. INTRODUCTION

Magnesium (Mg) has excellent uptake and release properties, but it has low hydrogen uptake and release rates. To raise the hydrogen uptake and release rates of Mg, transition metals like Pd [1], Cu [2], Co, Ni or Fe [3,4], and Ti [5], rare-earth metals such as La and Y [6], graphite [7,8], or intermetallic compounds such as Mg_2Ni, $LaNi_5$, and FeTi [9-11] have been added to Mg.

Carbon materials have been doped to Mg in some studies. Huot *et al*. [7] could prepare a metallic hydride rapidly by milling Mg with graphite at a high temperature under hydrogen pressure. They were able to synthesize the hydride by milling a mixture of Mg + 5 at% V + graphite at 573 K in 4 bar H_2 for 1 h. 2 wt% of either multiwall carbon nanotubes or graphite was admixed with Mg to prepare pelletized porous composites of Mg by Popilevsky *et al*. [8]. They reported that co-milling for 4 h of Mg with 2 wt% of carbon nanotubes and then pelletizing led to the best combination of hydrogen desorption kinetics, thermal conductivity, and mechanical stability [8]. Imamura *et al*. [12] milled mechanically Mg, graphite, and organic additive (benzene, cyclohexene or cyclohexane). In the obtained nanocomposites, mechanical milling caused the graphite structure to be decomposed to form many dangling carbon bonds in the graphite. The hydrogen absorbed in these nanocomposites existed as a C-H bond type in graphite and as hydride type in Mg.

Graphite has the average specific gravity (1.6-2.0) smaller than the specific gravity of aluminium, and the specific surface area of graphite is large.

In the present work, graphene was chosen as an

*Corresponding Author: Myoung Youp Song
[Tel: +82-63-270-2379, E-mail: songmy@jbnu.ac.kr]

additive to improve the hydrogen uptake and release properties of Mg. Five weight percent of graphene was added to pre-milled Mg by milling in hydrogen (reaction-involving milling). The hydrogen uptake and release properties of the graphene-added Mg were investigated.

2. EXPERIMENTAL DETAILS

Pure Mg powder (-20 + 100 mesh, 99.8%, metals basis, Alfa Aesar) and graphene (3-10 multi-layer graphene, 5-10 μm, purity ≥99 wt%, thickness nanometer 3-6 nm, surface area 150 m^2/g, chemical exfoliation proprietary method, Carbon Nano-material Technology Co., LTD) were used as starting materials.

Reaction-involving milling refers to the milling of a material in a reactive gas atmosphere. In this work, the reaction-involving milling was carried out in a hydrogen atmosphere. In the present work, milling in hydrogen to obtain the final samples is named as reaction-involving milling, and milling in hydrogen before reaction-involving milling to obtain the final sample is named as pre-milling.

Pre-milling of Mg was performed in a planetary ball mill (Planetary Mono Mill; Pulverisette 6, Fritsch). Samples with the desired compositions (total weight = 8 g) were mixed in a hermetically sealed stainless steel container with 105 hardened steel balls (total weight = 360 g); the sample to ball weight ratio was 1/45. All sample handling was performed in a glove box under Ar in order to prevent oxidation. The disc revolution speed was 400 rpm. The mill container (volume of 250 mL) was then filled with high purity hydrogen gas (~12 bar). Pre-milling of Mg was performed for 24 h, during which the mill container was refilled with hydrogen every two hours. The addition of graphene was also performed in a planetary ball mill (Planetary Mono Mill; Pulverisette 6, Fritsch). 95 wt% Mg (pre-milled for 24 h) + 5 wt% graphene (total weight = 8 g) were milled for 30 min under the conditions similar to those for the pre-milling of Mg. The prepared sample was named Mg-5graphene.

The quantity of absorbed or released hydrogen was measured as the reaction time passes using the Sieverts' type hydrogen uptake and release apparatus described previously [13]. 0.5 g of the samples was put into the reactor for these measurements.

Samples after reaction-involving milling and after hydrogen uptake-release cycling were characterized by X-ray diffraction (XRD) with Cu Kα radiation, using a Rigaku D/MAX 2500 powder diffractometer. The microstructures of the powders were observed using a JSM-5900 scanning electron microscope (SEM) operated at 20 kV. Raman spectrum measurements were performed with a NTEGRA (NT-MDT, Russia) Raman microscope with a laser excitation wavelength of 532 nm.

3. RESULTS AND DISCUSSION

Graphene is an allotrope of carbon and consists of carbon atoms arranged in a hexagonal lattice. Fig. 1 shows the XRD pattern of graphene and a SEM micrograph of graphene. Miller indices of the faces are marked in the XRD pattern of the graphene. Particle sizes were not homogeneous; some particles were very large and some were fine. The shapes of particles were very irregular; some particles were flat and some were rod-like.

Raman spectra of the graphene and as-prepared Mg-5graphene are shown in Fig. 2. Raman spectrum measurements were done with a laser excitation wavelength of 532 nm. The Raman spectrum of the graphene used in this work exhibited D, G, and 2D peaks, which can be assigned to graphene. The Raman shifts of the D, G, and 2D peaks for graphene were 1355, 1584, and 2713 cm^{-1}, respectively. The ratio of intensities of the D and G peaks, I_D/I_G, for graphene was 0.728. Ferrari *et al*. [14] reported that the shape and intensity of the 2D peak of graphene changed significantly compared with bulk graphite and the 2D peak of bulk graphite consists of two components $2D_1$ and $2D_2$. Ferrari *et al*. also reported that the graphene D peak is a single sharp peak, while in graphite it is a band consisting of two

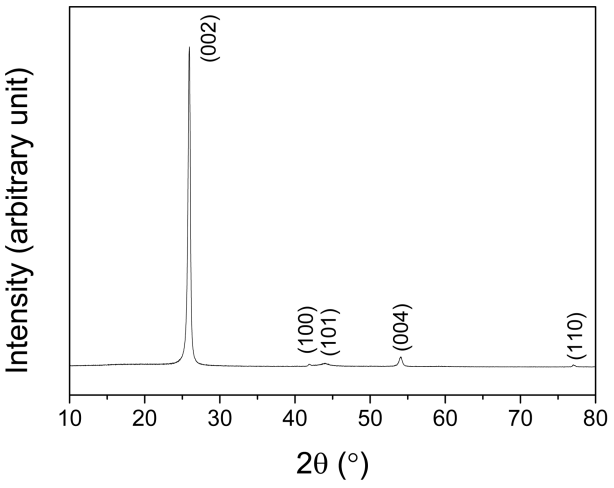

(a)

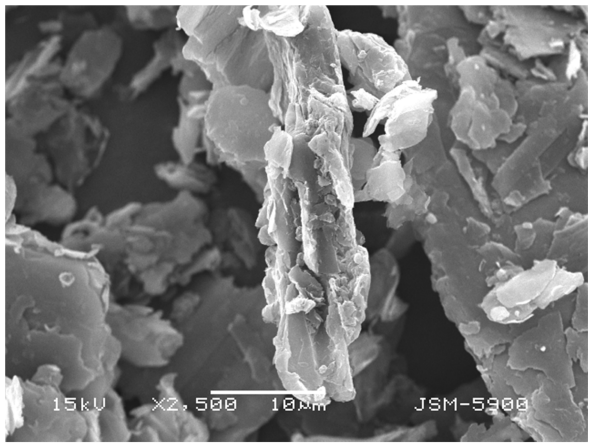

(b)

Fig. 1. (a) XRD pattern of graphene and (b) a SEM micrograph of graphene.

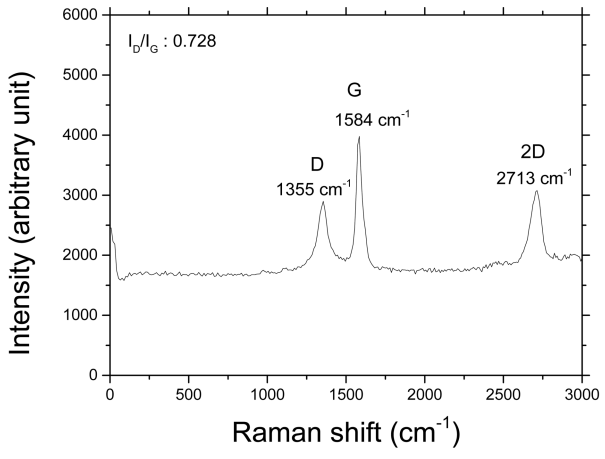

(a)

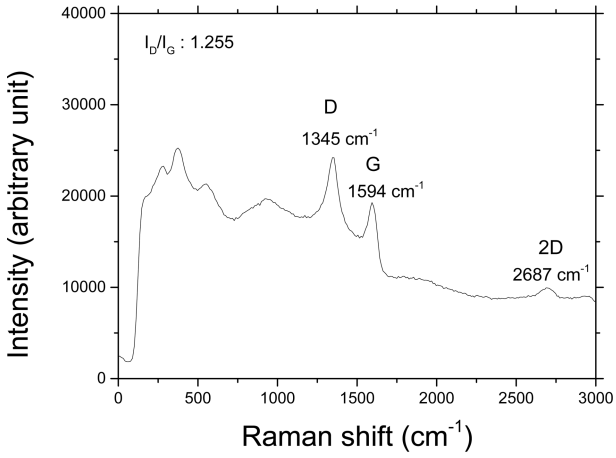

(b)

Fig. 2. Raman spectra of (a) graphene and (b) Mg-5graphene.

peaks, D_1 and D_2 [14]. The Raman spectrum in Fig. 2(a) shows that the material used in this work was not graphite but graphene. It was reported that the ratio of intensities of G and 2D peaks, $I_G/I_{2D,}$ is about 0.3 in single-layer and increases linearly until quintuple layers, and saturated in more than sextuple layers [15]. The graphene used in this work (Fig. 2(a)) had I_G/I_{2D} of 2.02, showing that the graphene used in this work was multilayer graphene. Hodkiewicz *et al* [16] reported that the D peak is known as the disorder band or the defect band and the intensity of the D peak is directly proportional to the level of defects in the sample. Rusi & S. R. Majid [17] reported that increments of I_D/I_G can be attributed to an increase in defects on the surface of the sample that were induced during the synthesis process. The ratio of intensities of D and G peaks, $I_D/I_{G,}$ for as-prepared Mg-5graphene was 1.255. The increase in I_D/I_G after reaction-involving milling of the pre-milled Mg with graphene shows that defects and disordering in the graphene were increased. As formation of the defects in graphene, we can consider the formation of point defects (vacancies) in the lattice points of the hexagonal basal plane. As disordering, we can consider the formation of stacking fault disorder and turbostratic graphite. In the graphene, stacking fault disorder is known to be generated due to forward shearing of the hexagonal basal planes after mechanical milling [18]. The

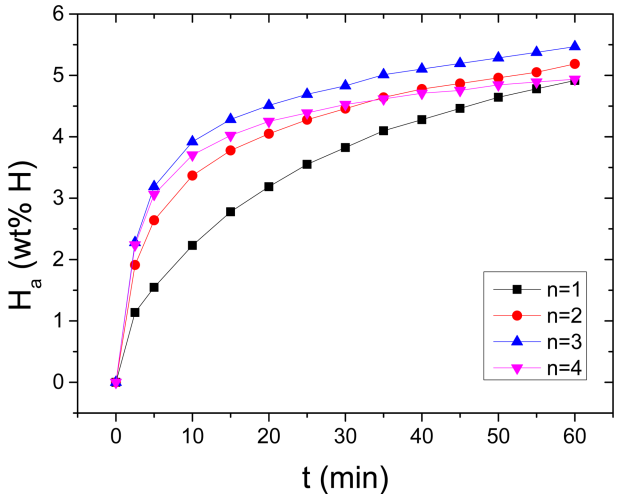

Fig. 3. Variation in H_a versus t curve with the number of cycles, n, for Mg-5graphene at 593K in 12 bar H_2.

turbostratic graphite is the graphene which has curled, twisted, and rotated planes [18]. Rather than the former (the formation of defects in graphene) since high energy is considered to be required to make vacancies in the lattice points of the hexagonal basal plane, we believe that, the latter (the generation of stacking fault disorder and the formation of turbostratic graphite) occurred after milling with the pre-milled Mg.

The quantity of hydrogen absorbed by the sample, H_a, was defined with respect to the sample weight. The quantity of hydrogen released by the sample, H_d, was also defined with respect to the sample weight. H_a and H_d were expressed as the units of wt% H.

Fig. 3 shows the variations in the H_a versus t curve with the number of cycles, n, at 593 K in 12 bar H_2 for Mg-5graphene. At n=1, the initial hydrogen uptake rate of Mg-5graphene was relatively high and the quantity of hydrogen absorbed for 60 min, H_a (60 min), was relatively large. The initial hydrogen uptake rate and the H_a (60 min) of Mg-5graphene increased as n increased from one to three and decreased from n=3 to n=4. These results indicate that the activation of Mg-5graphene was completed after n=2. At n=1, Mg-5graphene absorbed 1.14 wt% H for 2.5 min, 2.23 wt% H for 10 min, and 4.92 wt% H for 60 min. At n=3, Mg-5graphene absorbed 2.28 wt% H for 2.5 min, 3.92 wt% H for 10 min, and 5.47 wt% H for 60 min. Table 1 presents the variations in H_a with t at 593 K in 12 bar H_2 at n=1-4 for Mg-5graphene.

Table 1. Variations in the H_a (wt% H) with t at 593 K in 12 bar H_2 at n=1-4 for Mg-5graphene.

	2.5 min	5 min	10 min	30 min	60 min
n=1	1.14	1.55	2.23	3.82	4.92
n=2	1.91	2.64	3.37	4.46	5.19
n=3	2.28	3.19	3.92	4.83	5.47
n=4	2.24	3.06	3.70	4.53	4.94

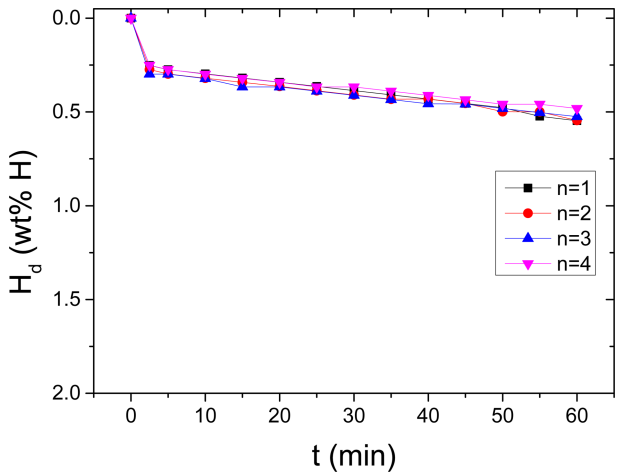

Fig. 4. Variation in H_d versus t curve with the number of cycles for Mg-5graphene at 593K in 1.0 bar H_2.

We define the effective hydrogen-storage capacity as the quantity of hydrogen absorbed for 60 min. Mg-5graphene had a high effective hydrogen-storage capacity of 5.47 wt% at 593 K in 12 bar H_2 at n=3.

The variation in the H_d versus t curve with the number of cycles for Mg-5graphene at 593 K in 1.0 bar H_2 is shown in Fig. 4. The H_d versus t curve exhibited a momentary hydrogen release of 0.25-0.27 wt% in the beginning. This is believed to be caused by the hydrogen desorbed from the surfaces of the particles and released from the MgH_2-H solid solution. We believe that the quantity of hydrogen released from the MgH_2-H solid solution is smaller than that from the surfaces of the particles, since it has been reported that the quantity of hydrogen contained in the MgH_2-H solid solution is small [19]. The hydrogen release rates were low, and the quantity of hydrogen released for 60 min, H_d (60 min), was

Table 2. Variations in the H_d (wt% H) with t at 593 K in 1.0 bar H_2 at n=1-4 for Mg-5graphene.

	2.5 min	5 min	10 min	30 min	60 min
n=1	0.25	0.27	0.30	0.39	0.55
n=2	0.27	0.30	0.32	0.41	0.55
n=3	0.27	0.30	0.32	0.41	0.53
n=4	0.25	0.30	0.30	0.39	0.50

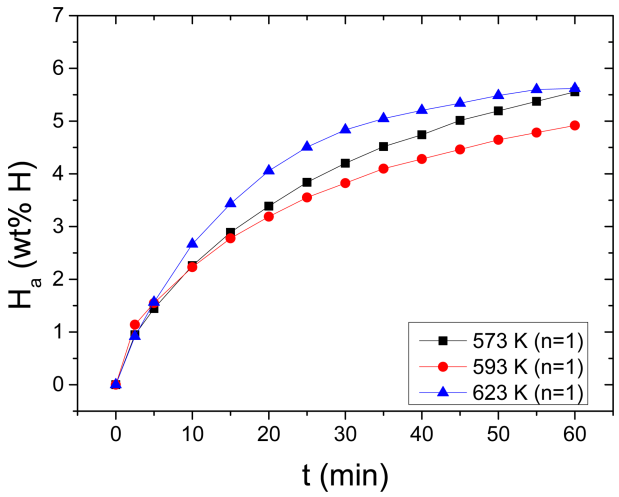

Fig. 5. H_a versus t curves at 573 K, 593 K, and 623 K in 12 bar H_2 for Mg-5graphene at n=1.

Table 3. Variations in H_a (wt% H) with t at 573 K, 593 K, and 623 K in 12 bar H_2 for Mg-5graphene at n=1.

	2.5 min	5 min	10 min	30 min	60 min
573 K	0.95	1.44	2.26	4.20	5.55
593 K	1.14	1.55	2.23	3.82	4.92
623 K	0.92	1.57	2.67	4.83	5.62

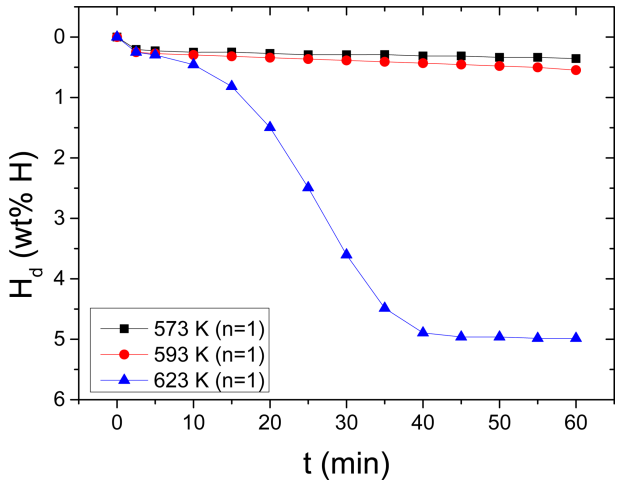

Fig. 6. H_d versus t curves at 573 K, 593 K, and 623 K in 1.0 bar H_2 for Mg-5graphene at n=1.

small. The H_d versus t curves were very similar. It is believed that the hydrogen release rates were low because the nucleation of the MgH_2-H solid solution occurred slowly. Future study will be performed to increase the nucleation rate of the MgH_2-H solid solution in Mg-5graphene. As n increased from one to four, H_d (60 min) decreased in general. At n=1, Mg-5graphene released 0.25 wt% H for 2.5 min, 0.30 wt% H for 10 min, and 0.55 wt% H for 60 min. Table 2 shows the variations in the H_d with t at 593 K in 1.0 bar H_2 at n=1-4 for Mg-5graphene.

Fig. 5 shows the H_a versus t curves at 573 K, 593 K, and 623 K in 12 bar H_2 for Mg-5graphene at n=1. The initial uptake rate increased from 573 K to 593 K and decreased from 593 K to 623 K, but they were similar at 573 K, 593 K, and 623 K. H_a (60 min) decreased as the temperature increased from 573 K to 593 K and increased from 593 K to 623 K. At 623 K, Mg-5graphene absorbed 0.92 wt% H for 2.5 min, 2.67 wt% H for 10 min, and 5.62 wt% H for 60 min. Table 3 shows the variations in H_a with t at 573 K, 593 K, and 623 K in 12 bar H_2 for Mg-5graphene at n=1.

The H_d versus t curves at 573 K, 593 K, and 623 K in 1.0 bar H_2 for Mg-5graphene at n=1 are shown in Fig. 6. The quantities of hydrogen released momentarily in the beginning were similar from 573 K to 623 K. The hydrogen release rates at 573 K and 593 K were low. H_d (60 min) increased as the temperature increased from 573 K to 623 K. The H_d versus t curve at 623 K was S-shaped, indicating that the hydrogen release reaction progressed by a nucleation and growth mechanism. The initial hydrogen release rate was relatively low and the hydrogen release rate was the highest at about 25 min. At 573 K, Mg-5graphene released 0.21 wt% H for 2.5 min, 0.25 wt% H for 10 min, and 0.36 wt% H for 60 min. At 623 K, Mg-5graphene released 0.25 wt% H for 2.5 min, 0.46 wt% H for 10 min, and 4.99 wt% H for 60 min. Table 4 shows the variations in the H_d with t at 573 K, 593 K, and 623 K in 1.0 bar H_2 for Mg-

Table 4. Variations in the H_d (wt% H) with t at 573 K, 593 K, and 623 K in 1.0 bar H_2 for Mg-5graphene at n=1.

	2.5 min	5 min	10 min	30 min	60 min
573 K	0.21	0.23	0.25	0.29	0.36
593 K	0.25	0.27	0.30	0.39	0.55
623 K	0.25	0.30	0.46	3.60	4.99

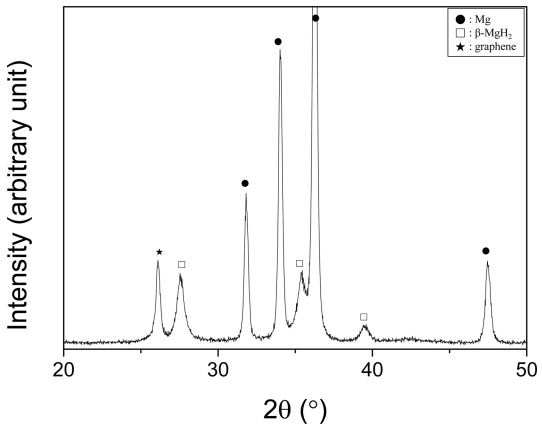

Fig. 7. XRD pattern of Mg-5graphene after reaction-involving milling.

5graphene at n=1.

Figure 7 shows the XRD pattern of Mg-5graphene after reaction-involving milling. The Mg-5graphene after reaction-involving milling contained a large amount of Mg and small amounts of β-MgH_2 and graphene. This shows that β-MgH_2 formed by the reaction of Mg with H_2 during grinding in hydrogen. β-MgH_2 is a low pressure form of magnesium hydride with a tetragonal structure. The Mg-5graphene dehydrogenated at the 4th hydrogen uptake-release cycle contained a large amount of Mg, a small amount of graphene, and very small amounts of β-MgH_2 and MgO. A very small amount of MgO is considered to have been formed by the reaction of Mg with oxygen adsorbed on the particle surfaces while treating the samples to obtain the XRD patterns.

SEM micrographs of Mg-5graphene after reaction-involving milling and Mg-5graphene dehydrogenated at the 4th hydrogen uptake-release cycle are shown in Fig. 8. Mg-5graphene after reaction-involving milling had no homogeneous particle size and its particles had some cracks, and the particle surfaces were undulated. Mg-5graphene dehydrogenated at the 4th hydrogen uptake-release cycle had a microstructure similar to that of Mg-5graphene after reaction-involving grinding. However, the particles of Mg-5graphene dehydrogenated at the 4th hydrogen uptake-release cycle had more cracks than those of Mg-5graphene after reaction-involving milling. The particles of Mg-5graphene dehydrogenated at the 4th hydrogen uptake-release cycle had some fine particles on their surfaces. The formation of cracks and fine particles with hydrogen absorption-release cycling are considered to result from the expansion and contraction of Mg with hydrogen uptake-release cycling.

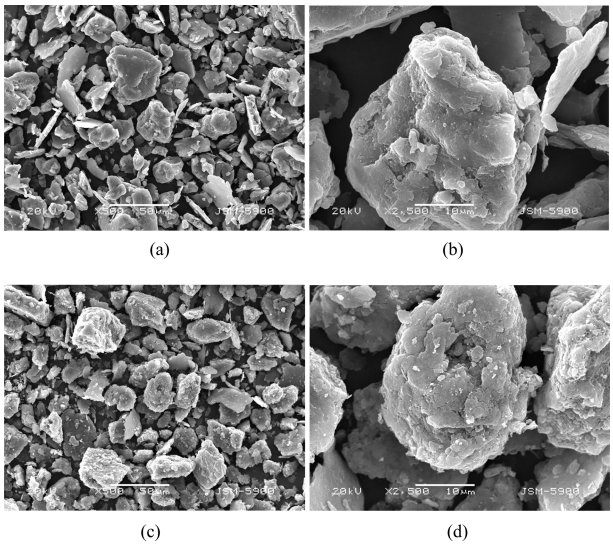

Fig. 8. SEM micrographs of Mg-5graphene (a, b) after reaction-involving milling and (c, d) dehydrogenated at the 4th hydrogen uptake-release cycle.

Jang *et al.* [20] investigated the hydrogen behaviors of MgH_x-5 and 10 wt% graphene composites prepared by reactive mechanical grinding. The available hydrogen storage amount for the MgH_x-5 wt% graphene composite was 5.09 wt% at 523 K. They reported that graphene was found to play the role of absorbent to store hydrogen, as well as playing the role of catalyst.

Figure 3 shows that the initial hydrogen uptake rate and the H_a (60 min) of Mg-5graphene increased from n=1 to n=3 and decreased from n=3 to n=4. The effects of hydrogen uptake-release cycling are the formation of cracks on the surfaces of particles from the

expansion and contraction of the particles and the coalescence of cracks inside particles due to maintenance at relatively high temperatures. It is believed that from n=1 to n=3, the initial hydrogen uptake rate and H_a (60 min) of Mg-5graphene increased since the effect of the formation of cracks was greater than that of the coalescence of cracks inside particles, and they decreased from n=3 to n=4 since the effect of the coalescence of cracks inside particles predominates over that of the formation of cracks.

Pre-milling of the Mg is believed to have created defects (facilitating nucleation), produced cracks and clean surfaces (leading to an increase in reactivity), and decreased particle sizes (leading to a reduction in diffusion distances, or an increase in the flux of the diffusing hydrogen atoms) [21-29]. Adding graphene, which has a large specific surface area, to the pre-milled Mg is believed to have decreased particle sizes as graphene filled the cracks of the Mg particles and helped separate the particles.

The hydrogen uptake-release cycling is also believed to have created defects, produced cracks and clean surfaces, and decreased particle sizes due to the expansion (by hydrogen uptake) and contraction (by hydrogen release) of Mg.

4. CONCLUSIONS

Pre-milling of Mg (for 24 h) and then adding graphene by milling in hydrogen (for 30 min) (named Mg-5graphene) significantly increased the hydrogen uptake and release rates, and the quantities of hydrogen absorbed and released for 60 min, of the Mg and graphene composite. The activation of Mg-5graphene was completed after n=2. Mg-5graphene had a high effective hydrogen-storage capacity of 5.47 wt% at 593 K in 12 bar H_2 at n=3. Mg-5graphene released 0.25 wt% H for 2.5 min and 4.99 wt% H for 60 min in 1.0 bar H_2 at 623 K at n=1. The increase in I_D/I_G, the ratio of intensities of the D and G peaks in the Raman spectra, after reaction-involving milling of the pre-milled Mg with graphene, compared with that of the used graphene, suggests that defects and disordering in the graphene were increased. We believe that the generation of stacking fault disorder and the formation of turbostratic graphite in graphene occurred after milling with the pre-milled Mg, rather than the formation of defects in graphene. Pre-milling of the Mg is believed to have created defects (facilitating nucleation), produced cracks and clean surfaces (leading to an increase in reactivity), and decreased particle sizes (leading to a reduction in diffusion distances, or an increase in the flux of the diffusing hydrogen atoms). Adding graphene, which has a large specific surface area, to the pre-milled Mg is believed to have decreased particle sizes as graphene filled the cracks of the Mg particles and helped separate the particles. The hydrogen uptake-release cycling is also believed to have created defects, produced cracks and clean surfaces, and decreased particle sizes due to the expansion (by hydrogen uptake) and contraction (by hydrogen release) of Mg.

ACKNOWLEDGEMENTS

This research was supported by Basic Science Research Program through the National Research Foundation of Korea (NRF) funded by the Ministry of Education (grant number NRF-2017R1D1A1B03030515).

REFERENCES

1. A. Krozer, B. Kasemo, *J. Phys.: Condens. Matter* **1**, 1533 (1989).
2. A. Karty, J. G. Genossar, and P. S. Rudman, *J. Appl. Phys.* **50**, 7200 (1979).
3. J.-L. Bobet, E. Akiba, Y. Nakamura, and B. Darriet, *Int. J. Hydrogen Energy* **25**, 987 (2000).
4. J. J. Reilly and R. H. Wiswall, *Inorg. Chem.* **7**, 2254 (1968).
5. M. Calizzi, D. Chericoni, L. H. Jepsen, T. R. Jensen, and L. Pasquini, *Int. J. Hydrogen Energy* **41**, 14447 (2016).
6. N. E. Tran, M. A. Imam, and C. R. Feng, *J. Alloy. Compd.* **359**, 225 (2003).
7. J. Huot, M.-L. Tremblay, and R. Schulz, *J. Alloy. Compd.* **356-357**, 603 (2003).
8. L. Popilevsky, V. M. Skripnyuk, M. Beregovsky, M.

Senzen, Y. Amouyal, and E. Rabkin, *Int. J. Hydrogen Energy* **41**, 14461 (2016).
9. L. Guoxian, W. Erde, and F. Shoushi, *J. Alloy. Compd.* **223**, 111 (1995).
10. G. Lian, S. Boily, J. Huot, A. van Neste, and R. Schulz, *J. Alloy. Compd.* **268**, 302 (1998).
11. M. Khrussanova, J.-L. Bobet, M. Terzieva, B. Chevalier, D. Radev, P. Peshev, and B. Darriet, *J. Alloy. Compd.* **307**, 283 (2000).
12. H. Imamura, M. Kusuhara, S. Minami, M. Matsumoto, K. Masanari, Y. Sakata, K. Itoh, and T. Fukunaga, *Acta Mater.* **51**, 6407 (2003).
13. M. Y. Song, S. H. Baek, J.-L. Bobet, J. Song, and S.-H. Hong, *Int. J. Hydrogen Energy* **35**, 10366 (2010).
14. A. C. Ferrari, J. C. Meyer, V. Scardaci, C. Casiraghi, M. Lazzeri, F. Mauri, S. Piscanec, D. Jiang, K. S. Novoselov, S. Roth, and A. K. Geim, *Phys. Rev. Lett.* **97**, 187401 (2006).
15. https://www.nanophoton.net/applications/22.html
16. https://tools.thermofisher.com/content/sfs/brochures/D19505~.pdf
17. Rusi & S. R. Majid, Scientific Reports volume 5, Article number: 16195 (2015).
18. R. A. Varin, T. Czujko, and Z. S. Wronski, *Nanomaterials for Solid State Hydrogen Storage*, pp. 301-302, Springer (2009).
19. J. F. Stampfer Jr., C. E. Holley Jr., and J. F. Suttle, *J. Amer. Chem. Soc.* **82**, 3504 (1959).
20. M.-H. Jang, S.-H. Park, and T.-W. Hong, *Korean J. Met. Mater.* **54**, 288 (2016).
21. S.-H. Hong and M. Y. Song, *Met. Mater. Int.* **22**, 544 (2016).
22. M. Y. Song, Y. J. Kwak, S. H. Lee, H. R. Park, *Met. Mater. Int.* **21**, 208 (2015).
23. S.-H. Hong and M. Y. Song, *Met. Mater. Int.* **21**, 422 (2015).
24. Y. J. Kwak, S. H. Lee, D. R. Mumm, M. Y. Song, *Int. J. Hydrogen Energy* **40**, 11908 (2015).
25. Y. J. Kwak, S. N. Kwon, M. Y. Song, *Met. Mater. Int.* **21**, 971 (2015).
26. S.-H. Hong and M. Y. Song, *Korean J. Met. Mater.* **54**, 358 (2016).
27. S.-H. Hong and M. Y. Song, *Met. Mater. Int.* **22**, 544 (2016).
28. M. Y. Song, Y. J. Kwak, and H. R. Park, *Korean J. Met. Mater.* **54**, 503 (2016).
29. S. N. Kwon, H. R. Park, and M. Y. Song, *Korean J. Met. Mater.* **54**, 510 (2016).